

PROBING THE TRANSVERSE IMPEDANCE OF THE ESRF STORAGE RING

L. Farvacque, E. Plouviez. ESRF, Grenoble, France

Abstract

We have probed the transverse impedance of the ESRF storage ring using different methods and obtained data about the localisation and the frequency dependency of the impedance of our storage ring. We first used the local bump method [1]; it allowed us to accurately compare the impedance of various components of our ID straight sections: low gap vacuum chamber, scraper, in-vacuum undulator. We also used a method based on the measurement of the second derivative of the beam energy loss per turn with respect to its transverse position. Though this method has a much lower sensitivity than the previous one, it enabled to obtain information on the global transverse impedance of the whole machine at different frequencies of the spectrum from about 6 to 30 GHz. This frequency scan was obtained by applying the transverse beam position offset with the proper time shape, and measuring the beam energy loss per turn induced by this perturbation for various chromaticity settings. This paper describes our measurement set up and data analysis method and gives measurement results.

1 LOCAL IMPEDANCE PROBING

The vacuum chambers of the ID straight sections are responsible for a large part of the impedance of the ESRF storage ring, due to their reduced cross section. We used the method described by L. Emery et al in [1] to get quantitative data about the impedance of our different types of ID vacuum chambers as well as other components located in these straight sections and suspected of having a large impedance like the scrapers.

The principle of the local bump method is to create a local bump which will force the beam orbit to get closer to the vacuum chamber in the area where we want to probe the transverse impedance. Due to this orbit shift, the interaction of the imaginary part $\text{Im}Z_t$ with the beam current momentum $I\Delta z$ will induce a wake field which will give additional kicks to the tail of the beam,

$$\langle \Delta z' \rangle = -\frac{I_{av}\Delta z}{E} \int_0^\infty d\omega \text{Im} Z_T(\omega) |\rho(\omega)|^2 \quad (1)$$

with I_{av} =beam average current, $I_{av}\rho(\omega)$ =current spectrum and E =beam energy in eV. Due to these kicks, a closed orbit perfectly unperturbed outside the closed bump at zero current per bunch, will turn in an orbit slightly distorted by these wake fields when a beam with a high current per bunch is stored. We have measured this effect by a simple processing of data from the 224 BPMs of the storage ring.

2 MEASUREMENT METHOD

We have performed the following measurement sequence: with the 8 mA, 992 bunches beam, we have recorded the full storage ring closed orbit with closed bumps of opposite signs, using 224 BPMs; we have used the difference between these closed orbits recorded with opposite bumps as a reference vector CO_U . Figure 1 shows a plot of one part of such a set of records. The bump starts and ends in the middle of the achromat, extending over the whole cell and is parallel to the beam axis inside the straight section. We used vertical bumps to study the low gap ID vacuum chambers. We studied our scraper in both vertical and horizontal planes.

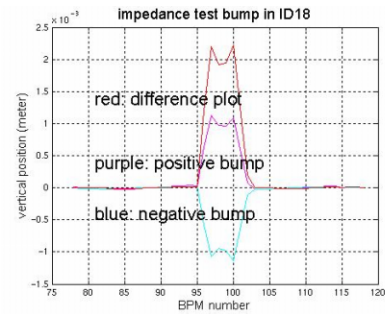


Figure 1: plot of the +/-1mm amplitude closed bumps used for local impedance measurements

We then filled the storage ring with a single 22nC bunch of the same average intensity and performed the same recording with the same closed bumps getting the vector CO_S . Between the uniform filling and single bunch recordings, no change were made to the optics settings, and no orbit correction was performed. We obtained the difference between the uniform filling difference record and the single bunch difference record: $CO_{WF}=CO_S-CO_U$. We then tried to calculate a fit of CO_{WF} using the orbit distortion that would be caused by a combination of two kicks located at the ends of the straight section.

3 FIT OF THE ORBIT DISTORTION MEASUREMENTS

Figure 2 shows the recording of CO_{WF} made on a 5m long / 8mm gap straight section vacuum chamber and the fit of this recording by the distortion produced by two kickers located at the end of the straight sections; the fit is excellent (blue=measurement, green=fit).

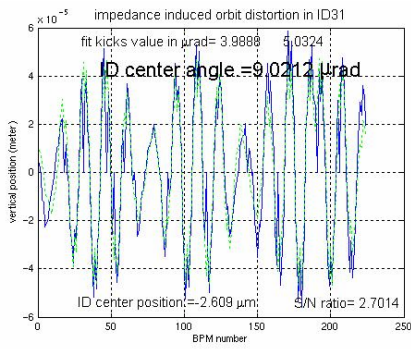


Figure 2: plot of the fit of the orbit distortion caused by the impedance of a 8mm gap 5m long straight section.

By performing 2 successive measurements with the same beam filling-bump combination separated by 20 minutes and a machine refill and comparing these recordings we estimated the resolution of our fit to .06μrad and 1.4 μm.

4 EFFECTIVE IMPEDANCE OF SOME COMPONENTS

Using the formalism presented in [1], which relates the additional focusing strength Kl of the wake fields, measured during our tests to the imaginary part of the effective transverse impedance $Im(Z_T)_{eff}$

$$(Kl) = q \frac{Im(Z_T)_{eff}}{2\sqrt{\pi}\sigma_t(E/e)} \quad (2)$$

we derived the value of $Im(Z_T)_{eff}$ of some of our machine components: the in vacuum undulator, the Cu/NEG coated 8mm gap and stainless steel 11 mm gap 5m long vacuum vessels and a scraper:

Components tested (22nC $\sigma_t = 55ps$ test bunch)	(Kl) (rad/m)	$Im(Z_T)_{eff}$ (KΩ/m)
2m long/6mm gap in vacuum ID	2.2 mrad	117
5m long/8mm gap vessel	4.5 mrad	239
5m long/11mm gap vessel	1.6 mrad	170
4mm opening scraper	1.4 mrad	149

5 BROAD BAND IMPEDANCE MEASUREMENTS

The static bump measurement method can give very accurate results; however, due to the limited bandwidth of the spectrum of our $\sigma_t = 55ps$ bunches, they do not give much information on the interaction of the beam with the broad band impedance. With the chromaticity used in single bunch operation the frequency span of interest can then extend from 10 to 30GHz due to the chromatic frequency shift. Measurements of the rise time of instabilities on the SR [2] at different chromaticities were fitted with a combination of resistive wall and broadband impedance model (this is the impedance model used in figure 4); and a good fit was obtained for a $Q=1$ broad band impedance with a 6.8 MΩ maximum value of βZ_T

at $f_c = 22GHz$. Time domain electromagnetic simulation of the SR components [3] also indicates a broad band impedance with a maximum at 20GHz, with similar values of βZ_T and f_c . We have tried to cross-check these results by using a method based on the measurement of the second derivative of the longitudinal impedance with respect to a vertical beam position offset, following an idea of A. Hofmann [4]. This parameter is related to the real part of the transverse impedance by:

$$Re Z_T(\omega) = c / 2\omega \cdot \partial^2 Z_L / \partial z^2 \quad (2)$$

Thus its measurement allows a direct probing of the real part of the transverse impedance at high frequencies if we use a beam offset $D = I \cdot \Delta z$ with the proper time shape for the test.

5.1 Measurement principle

It is possible to measure $\partial^2 Z_L / \partial z^2$ by applying a symmetrical $\pm \Delta z$ offset to the beam position, and by measuring the variation of the energy loss per turn due to the impedance change. The energy loss change induces a change $\Delta\Phi$ of beam the synchronous phase, and the change of this phase can be detected using a diagnostic tool implemented on the ESRF storage ring and called the beam phase monitor.

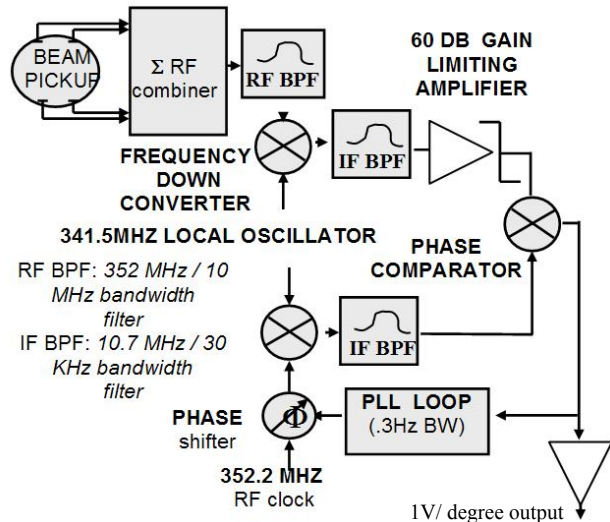


Figure 3: beam phase monitor layout

This diagnostic tool is a RF phase modulation receiver which compares the phase of a signal coming from a beam pick up to the phase of the SR RF drive signal. The design of this receiver, shown in the figure 3, is such that it removes all the position and intensity dependent modulation of the pick up signals and allows to detect oscillation of the beam phase in the 1KHz to 15KHz spectrum. The sensitivity of this receiver allows to detect phase modulation lower than 10^{-3} degrees when a proper signal processing such as a FFT analysis is applied. The effect of the variation of Z_L is a quadratic effect, so the effect of the effective transverse bunch spectrum interacting with the broad band impedance at very high

frequency will result in DC changes of the beam loss per turn. A gaussian bunch with $\sigma_{\tau}=40\text{ps}$ oscillating on the 0 transverse mode with a ξ chromaticity, will have the spectrum of $D=I\Delta z$ centered around a frequency equal to the chromatic frequency shift $f_{\xi}=19.4\text{GHz}$. ξ for the ESRF storage ring optics setting, and a bandwidth of about $\pm 4\text{GHz}$. The additional energy loss per turn due to a Δz amplitude transverse oscillation applied with a kicker located at s_K will be:

$$\Delta E = \int_0^{2\pi} ds \int_0^{\infty} d\omega \frac{D^2(\omega, s_k)}{4} \cdot \frac{\beta(s)}{\beta(s_k)} \frac{\partial^2 Z_L(\omega, s)}{\partial z^2} \quad (3)$$

5.2 Application of the oscillation

A damped single bunch oscillation on the mode 0 is started by applying a single turn kick. The oscillation amplitude will decay with the time constant given by the synchrotron radiation damping $\tau_{\perp}=7\text{ms}$ at the ESRF. This decay shall not be affected by the head tail effect if the loss of coherency due to the chromaticity is fast enough, which should be the case. We have also checked that the transverse position tune dependency is small enough to avoid spoiling the measurement. In order to get a measurable effect after averaging, we applied this kick at the fastest rate compatible with τ_{\perp} : we operated at $f_K=70\text{Hz}$. Thus a shift of the beam synchronous phase will appear and decay at the rate f_K , which will allow a sensitive detection of the effect by FFT. Due to this pulsed application of the transverse oscillation the amplitude of the oscillation of E at f_K is:

$$\Delta E_{f_K} \text{ rms} = \frac{\sqrt{2}}{2} f_K \frac{\tau_{\perp}}{2} \Delta E \quad (4)$$

We integrated numerically the expressions (3) and (4) for a broad band impedance with at $f_c=20\text{GHz}$ and $Q=1$ to get the energy loss per turn variation as a function of ξ , βZ_T , σ_{τ} , I and Δz , and compared these results to those of the measurement of the beam energy loss per turn. The expected beam phase oscillation amplitude is about 10^{-3} degree as shown in Figure 4.

5.2 Measurement results

We applied $.2\ \mu\text{rad}$ to $.4\ \mu\text{rad}$ test kicks to a single bunch with $\beta_K=4\text{m}$ at S_K , the location of S_K , with the repetition rate f_K . For different values of the beam current I , bunch length τ and kick amplitude A , we observed a line at f_K on the beam phase monitor output signal, with an amplitude dependency with respect to I , τ and A consistent with the effect of $\partial^2 Z_L / \partial z^2$. From applying the same kick to a beam of the same intensity with a multi bunch filling, we checked that the f_K line disappeared, a proof that we measured a single bunch effect with the single bunch filling. We also checked that the position dependant tune shift did not spoil our measurements, by recording data with various kick amplitudes. The line amplitude variation at a chromaticity lower than $.4$ was

modified by the head tail effect. For this reason, the impedance probing was only correct for $.47 < \xi < 1.3$. In this range, we also observed a decrease of the amplitude of the f_K line for the highest f_{ξ} value; this should be a sign that for these chromatic frequency shift of the beam transverse spectrum, the frequency range of the beam/impedance interaction was above the peak frequency of the broad band impedance. The fit with our measurements with the result of the computation of (3) and (4) indicates a peak value of βZ_T is $6.5\text{M}\Omega \pm 20\%$

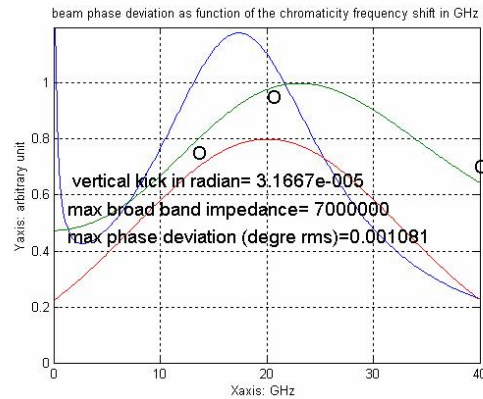


Figure 4: plot of the $\text{Re } \beta Z_T(\omega)$ function (blue), of the spectrum of $D=I\Delta z$ for $\xi=.45$ (red), of the predicted (green) and measured (O) amplitude of the $\Delta\Phi$ beam phase oscillation versus f_{ξ} , in GHz for our test kick. The vertical scale is arbitrary to fit the plot size.

6 CONCLUSION

We have performed measurements of the transverse impedance of the ESRF storage ring using the local bump method. We found that the high resolution of the BPM system and optics stability achieved at ESRF, as in most recent light sources, allowed an easy and accurate probing of the imaginary part of the straight section effective impedance. We have also developed a method allowing the measurement of the real part of the impedance at frequencies higher than 10 GHz and obtained a confirmation of the value of the broadband transverse impedance of our storage ring.

REFERENCE

- [1] L. Emery et al, "local bump method for measurement of transverse impedance of narrow gap ID chambers in storage rings", PAC 2001, Chicago, June 2001
- [2] R. Nagaoka et al, "Observation, analysis and cure of the transverse multibunch instability at ESRF", EPAC 2000, Vienna, June 2000
- [3] T. Gunzel, "Evaluation of the Vertical Transverse Impedance of the ESRF-machine by Element-wise Wakefield Calculation", This conference
- [4] A. Hofmann, "Transverse instabilities, head tail effect", CAS 2001 course, Sevilla, October 2001